Synthesis of $NiCo_2O_4$/Nano-ZSM-5 nanocomposite material with enhanced electrochemical properties for the simultaneous determination of ascorbic acid, dopamine, uric acid and tryptophan

Balwinder Kaur[a], Biswarup Satpati[b], and Rajendra Srivastava*[a]

Supporting Information

Chronoamperometry study

Chronoamperometry was used to calculate the diffusion coefficient (D) and rate constant (k) for the electro-catalytic reaction (Fig. S4-7). Chronoamperograms were obtained at different concentrations of analytes at a desired potential step (250, 400, 550, and 850 mV for AA, DA, UA, and Trp, respectively) (Fig. S4-7). The plots of I verses $t^{-1/2}$ exhibited straight lines for different concentrations of analytes (Fig. S4-7, inset a). Cottrell equation (Eq. 1) was used to calculate the diffusion coefficient for various analytes investigated in this study.[1]

$$I_p = n\,F\,A\,D^{1/2}\,c/\pi^{1/2}\,t^{1/2} \qquad (1)$$

Where I_p is the catalytic current of $NiCo_2O_4$ (30 %)/Nano-ZSM-5/GCE in the presence of analyte, F is the Faraday constant (96500 C/mole), A is the geometric surface area of the electrode (0.07 cm^2), D is the diffusion coefficient (cm^2/s), c is the analyte concentration (mol/cm^3), and t is the time elapsed (s). The diffusion coefficients for AA, DA, UA, and Trp, were found to be 2.2×10^{-4}, 8.4×10^{-4}, 4.3×10^{-4}, and 1.4×10^{-4} cm^2/s, respectively.

Chronoamperometry was also employed to calculate the rate constant (k) for electro-catalytic reaction through Eq. 2.[2]

$$I_C/I_L = \gamma^{1/2}\,[\pi^{1/2}\,\mathrm{erf}\,(\gamma^{1/2}) + \exp\,(-\gamma)/\gamma^{1/2}] \qquad (2)$$

Where I_C is the catalytic current of $NiCo_2O_4$ (30 %)/Nano-ZSM-5/GCE in the presence of analyte, I_L is the limiting current in the absence of analyte and $\gamma = kC_0t$ (C_0 is the bulk concentration of analyte) is the argument of the error function. In cases, where γ exceed 2, the error function is almost equal to 1 and the above equation can be reduced to:

$$I_C/I_L = \pi^{1/2}\,\gamma^{1/2} = \pi^{1/2}\,(kC_0t)^{1/2} \qquad (3)$$

Where k, C_0 and t are the catalytic rate constant (1/Ms), analyte concentration (M), and time elapsed (s), respectively. Eq. 3 can be used to calculate the rate constant of the catalytic process. Based on the slope of I_C/I_L vs. $t^{1/2}$ plot; k can be obtained for a given analyte concentration (Fig. S4-7, inset b). From the values of the slopes, an average value for k was obtained for the oxidation of analyte. The rate constants for electro-catalytic oxidation of AA, DA, UA, and Trp were found as 7.8×10^3, 8.3×10^3, 3.8×10^2, and 2.8×10^3 1/s M, respectively.

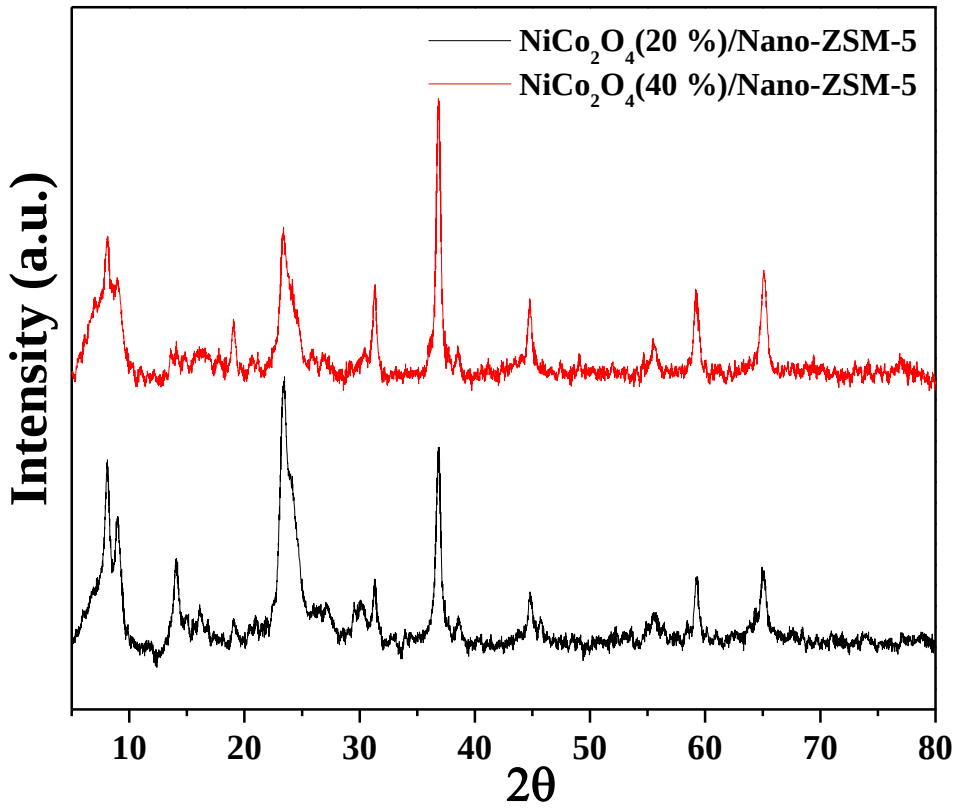

Fig. S1. XRD patterns of (a) $NiCo_2O_4$ (20 %)/Nano-ZSM-5 and (b) $NiCo_2O_4$ (40 %)/Nano-ZSM-5.

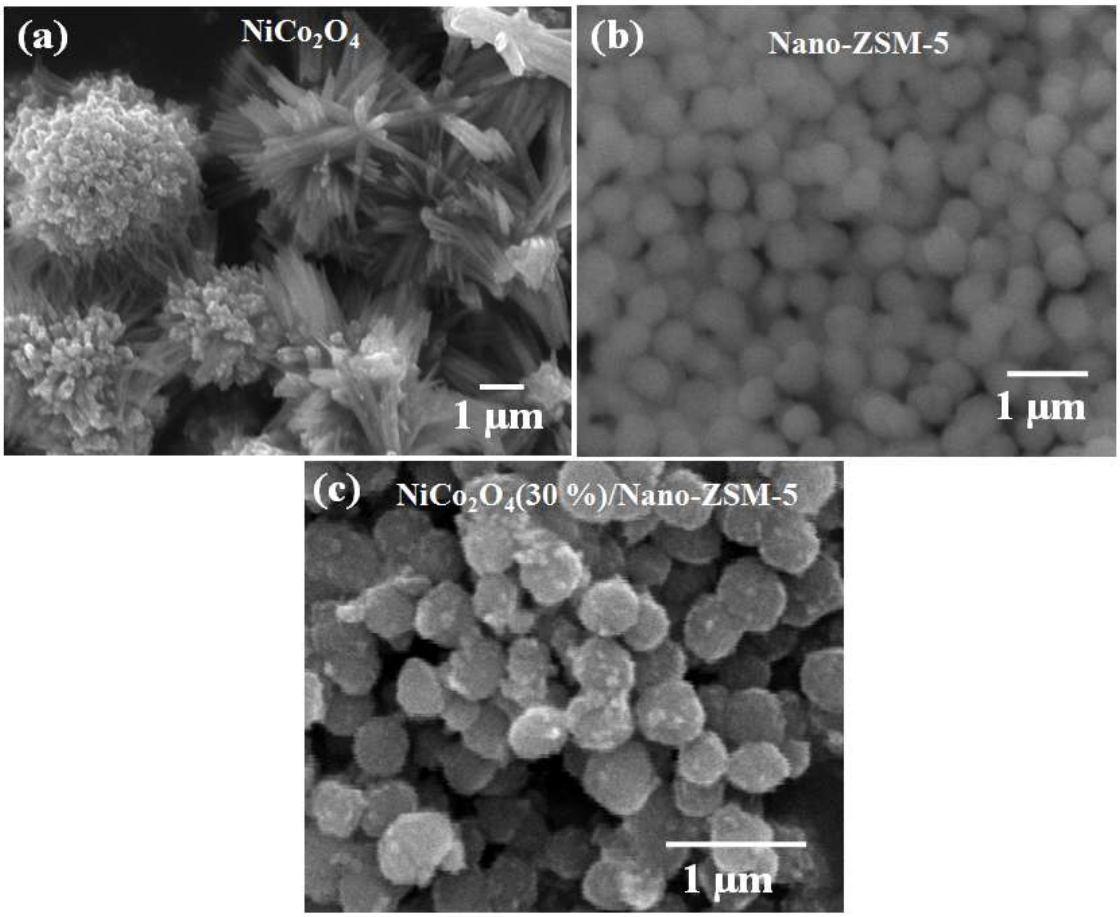

Fig. S2. SEM images of (a) $NiCo_2O_4$, (b) Nano-ZSM-5, and (c) $NiCo_2O_4$ (30 %)/Nano-ZSM-5.

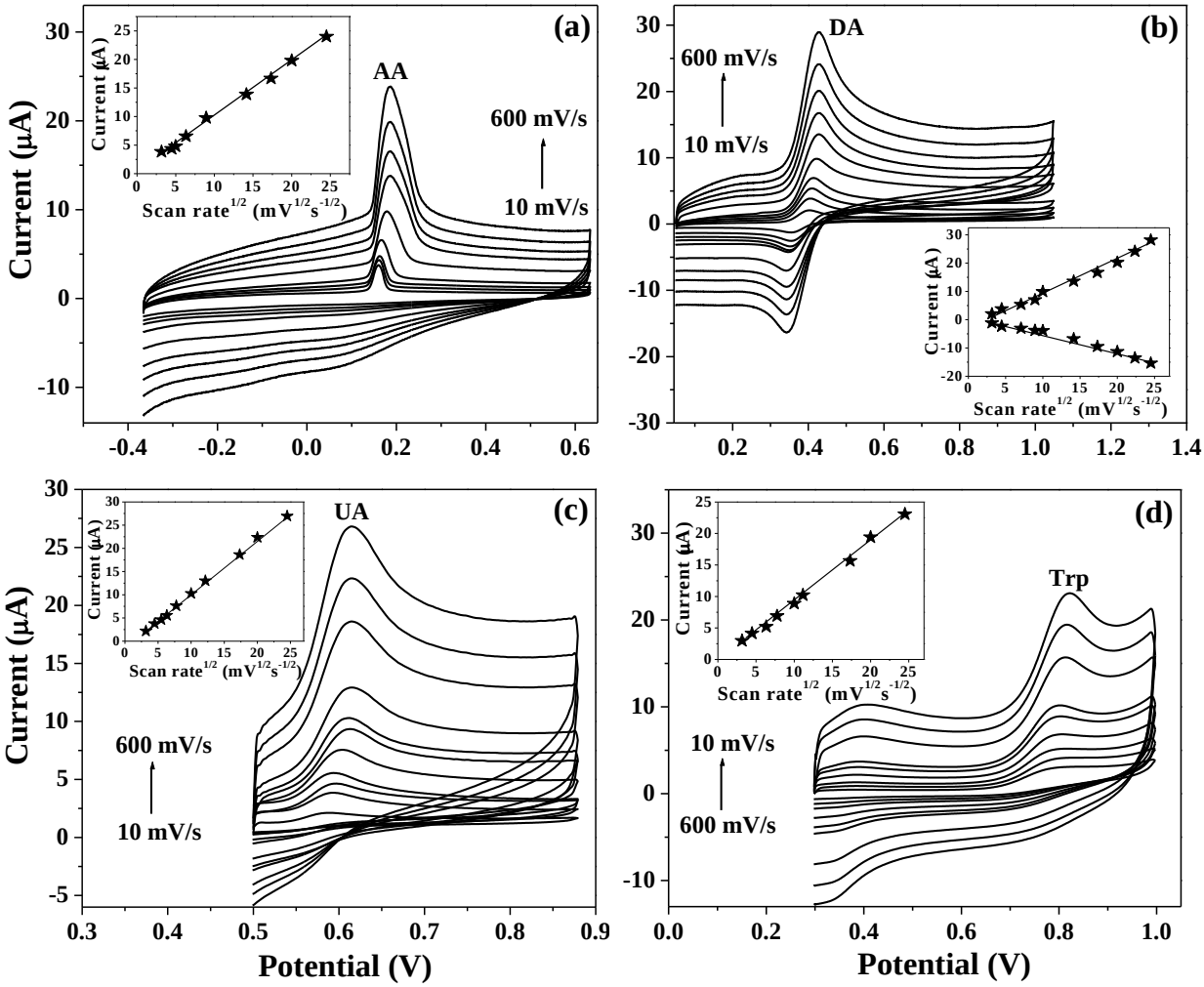

Fig. S3. CVs at $NiCo_2O_4$ (30 %)/Nano-ZSM-5/GCE containing (a) AA (10 μM), (b) DA (10 μM), (c) UA (10 μM), and (d) Trp (10 μM) in buffer solution (pH 3.5) at different scan rates (10–600 mV/s). Inset: plot of peak currents vs. square root of scan rates.

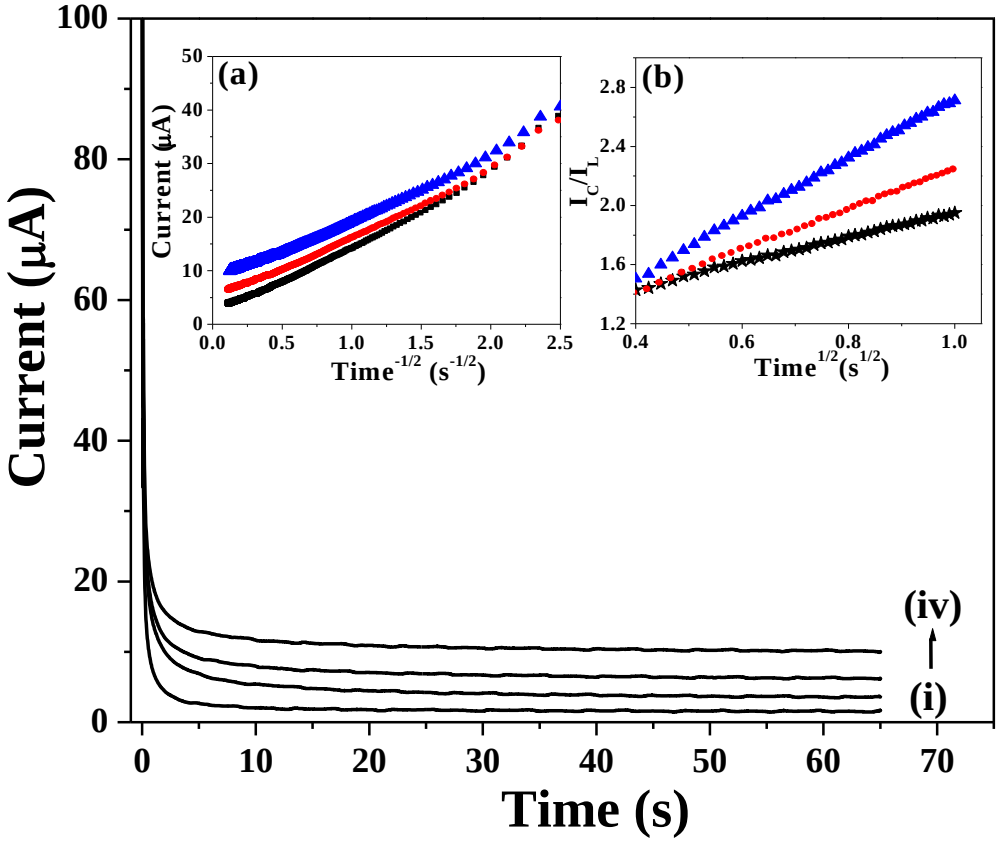

Fig. S4. Chronoamperograms obtained at $NiCo_2O_4$ (30 %)/Nano-ZSM-5/GCE (i) in the absence and in the presence of (ii) 50 μM, (iii) 80 μM, and (iv) 100 μM of AA in 10 mL buffer solution (pH 3.5). Inset: (a) Dependence of current on the time$^{-1/2}$ derived from the chronoamperogram data. (b) Dependence of I_C/I_L on time$^{1/2}$ derived from the data of chronoamperograms.

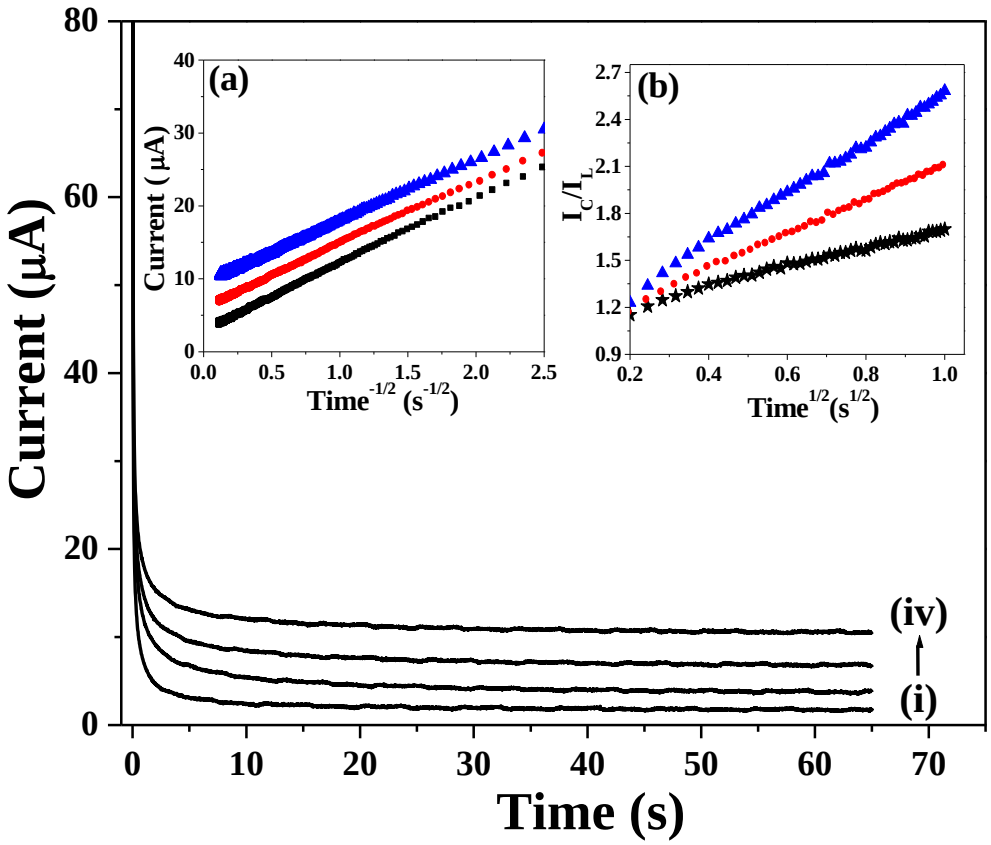

Fig. S5. Chronoamperograms obtained at $NiCo_2O_4$ (30 %)/Nano-ZSM-5/GCE (i) in the absence and in the presence of (ii) 50 μM, (iii) 80 μM, and (iv) 100 μM of DA in 10 mL buffer solution (pH 3.5). Inset: (a) Dependence of current on the time$^{-1/2}$ derived from the chronoamperogram data. (b) Dependence of I_C/I_L on time$^{1/2}$ derived from the data of chronoamperograms.

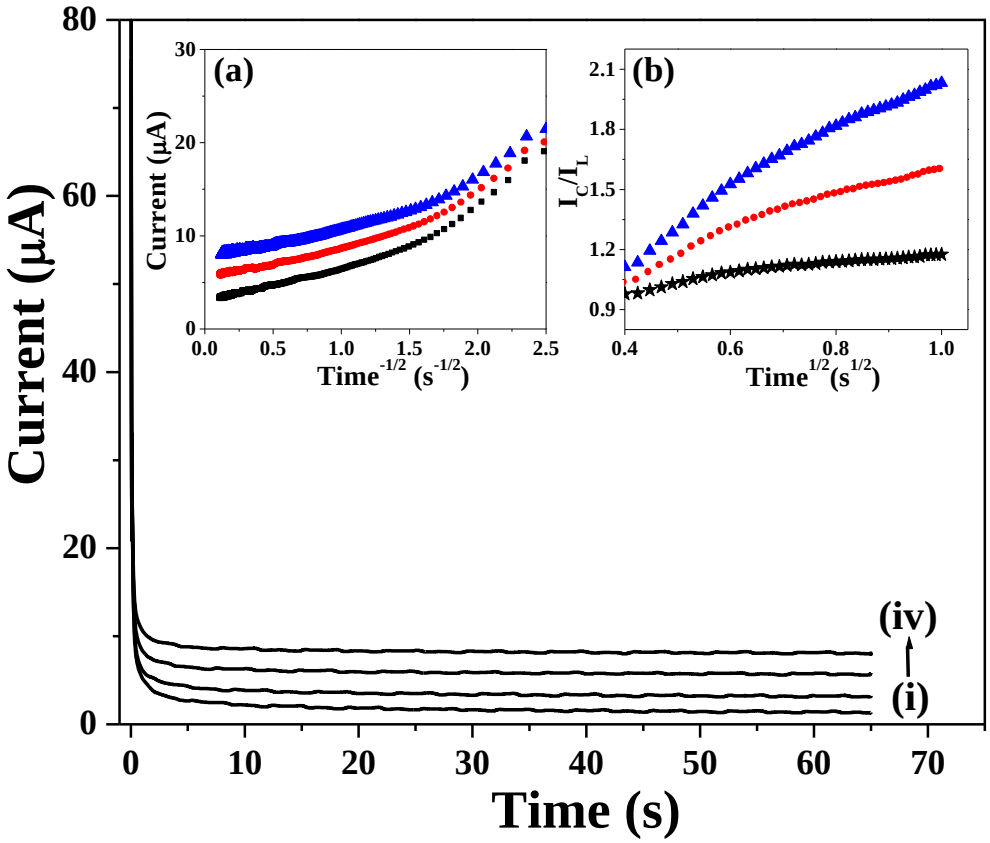

Fig. S6. Chronoamperograms obtained at $NiCo_2O_4$ (30 %)/Nano-ZSM-5/GCE (i) in the absence and in the presence of (ii) 50 μM, (iii) 80 μM, and (iv) 100 μM of UA in 10 mL buffer solution (pH 3.5). Inset: (a) Dependence of current on the time$^{-1/2}$ derived from the chronoamperogram data. (b) Dependence of I_C/I_L on time$^{1/2}$ derived from the data of chronoamperograms.

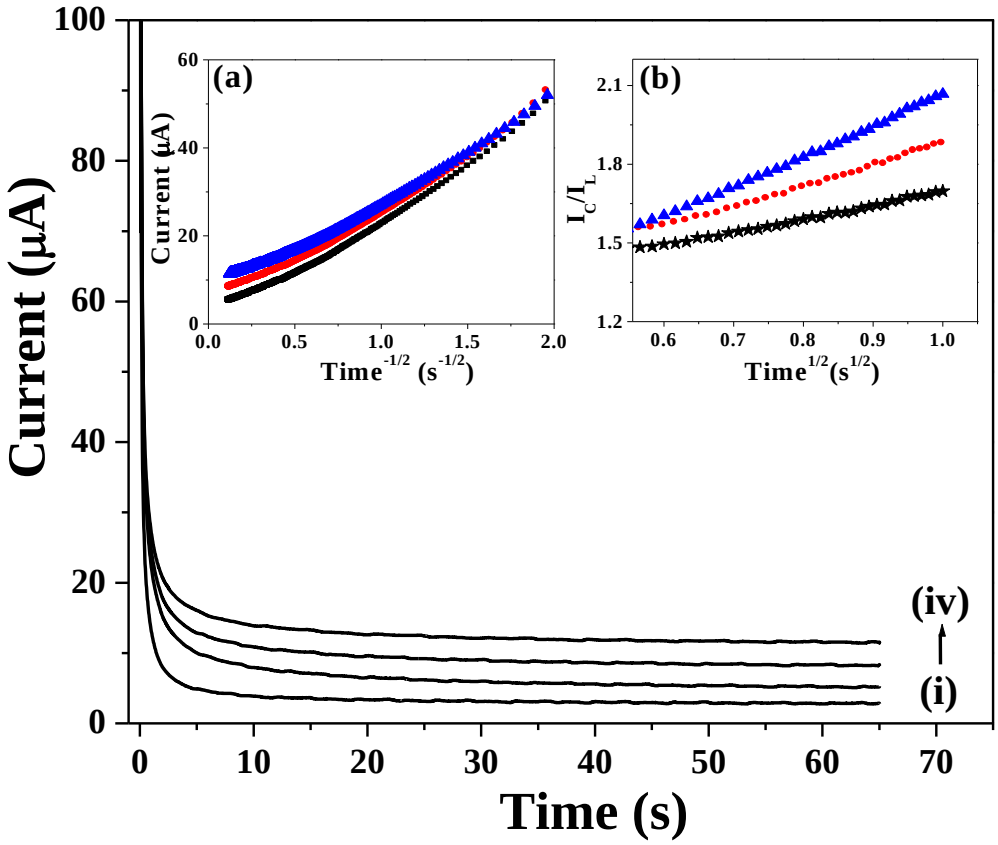

Fig. S7. Chronoamperograms obtained at $NiCo_2O_4$ (30 %)/Nano-ZSM-5/GCE (i) in the absence and in the presence of (ii) 50 μM, (iii) 80 μM, and (iv) 100 μM of Trp in 10 mL buffer solution (pH 3.5). Inset: (a) Dependence of current on the time$^{-1/2}$ derived from the chronoamperogram data. (b) Dependence of I_C/I_L on time$^{1/2}$ derived from the data of chronoamperograms.

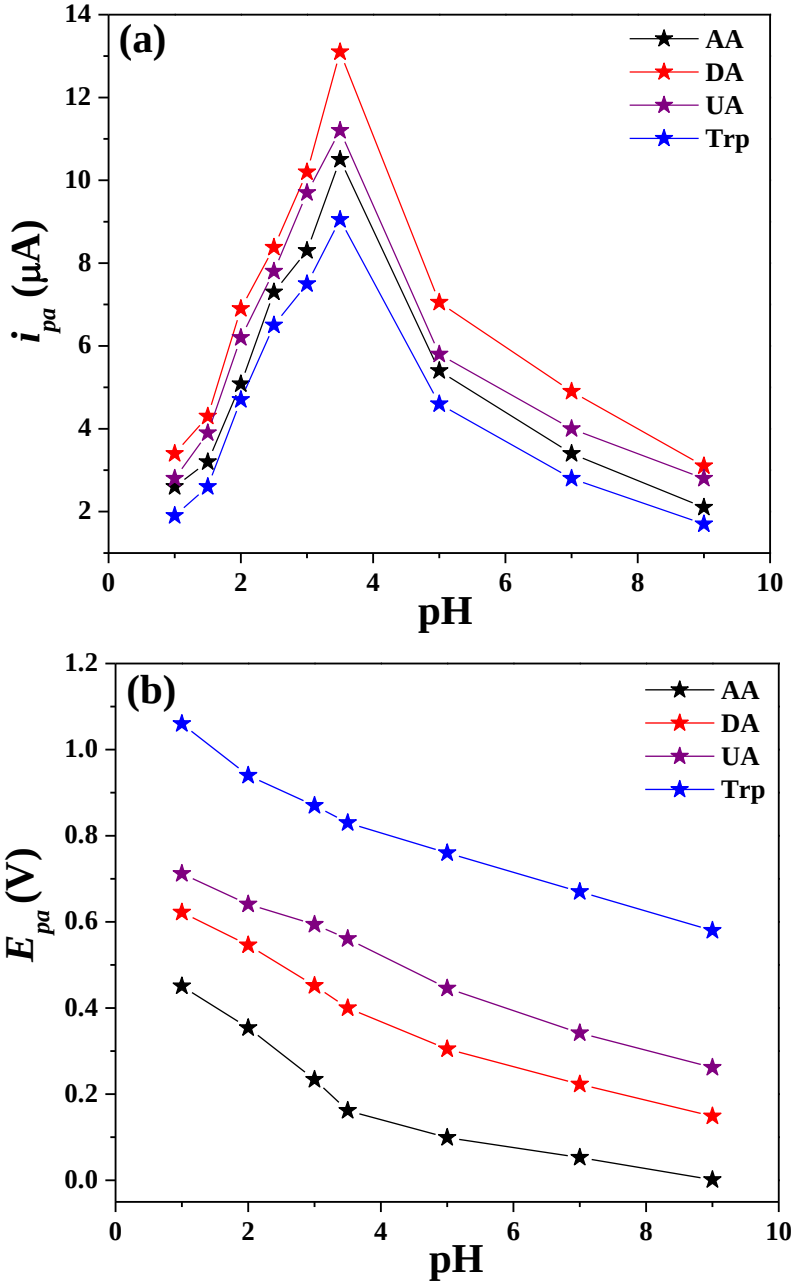

Fig. S8. Influence of the pH on (a) oxidation peak currents and (b) the peak potentials of AA, DA, UA, and Trp at a scan rate 20 mV/s.

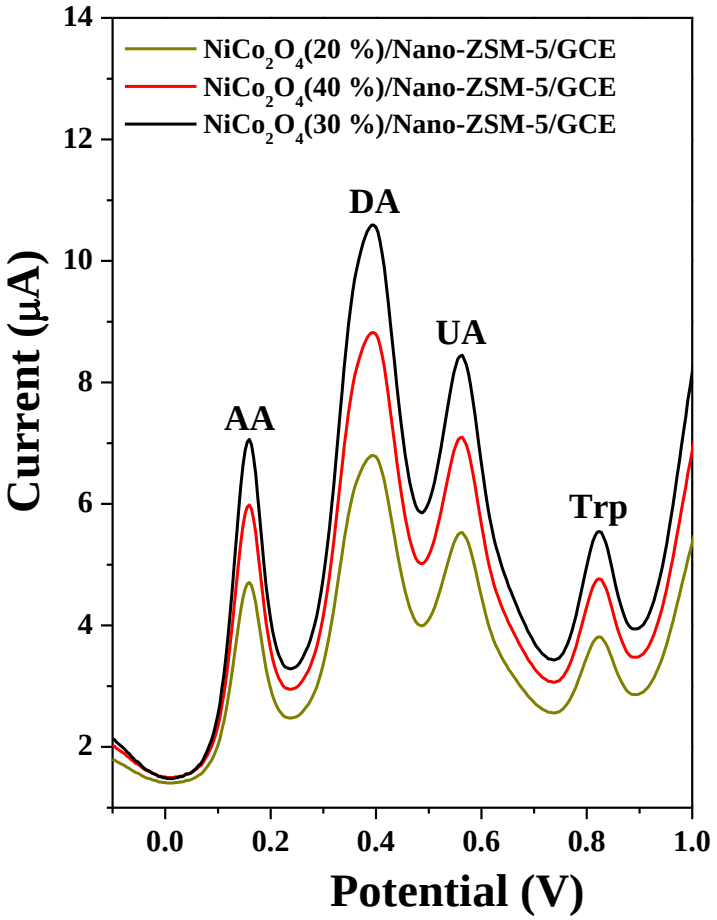

Fig. S9. Comparison of DPV of quaternary mixture containing (10 μM each) of AA, DA, UA, and Trp at various modified GCE ($NiCo_2O_4$ (20 %)/Nano-ZSM-5/GCE, $NiCo_2O_4$ (30 %)/Nano-ZSM-5/GCE, and $NiCo_2O_4$ (40 %)/Nano-ZSM-5/GCE in phosphate buffer solution (pH 3.5). DPV parameters were selected as: pulse amplitude: 50 mV, pulse width: 50 ms, scan rate: 20 mV/s.

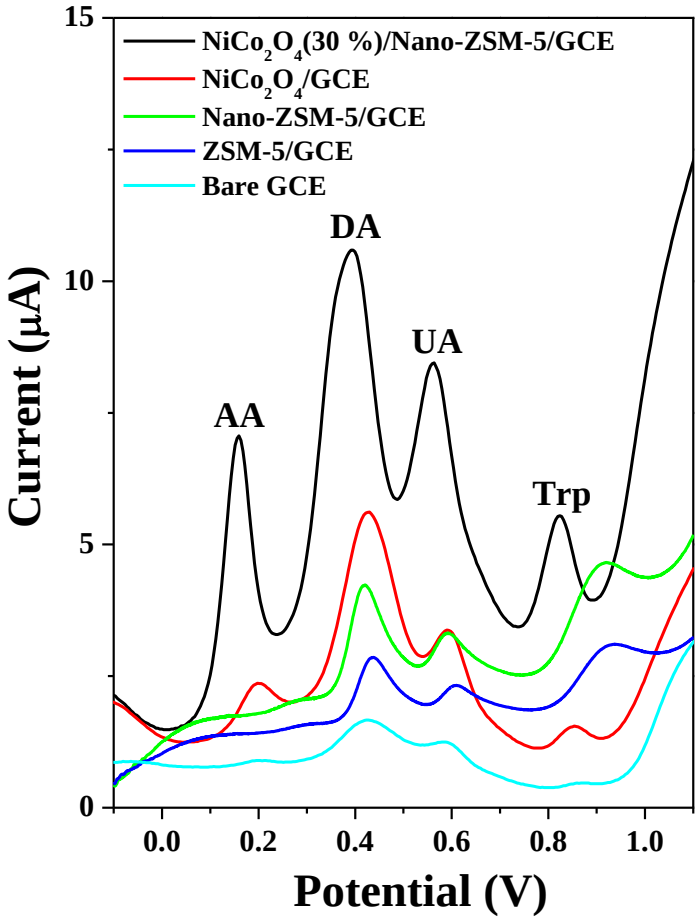

Fig. S10. Comparison of DPV of quaternary mixture containing (10 μM each) of AA, DA, UA, and Trp at different modified electrodes ($NiCo_2O_4$ (30 %)/Nano-ZSM-5/GCE, $NiCo_2O_4$/GCE, Nano-ZSM-5/GCE, ZSM-5/GCE) and bare GCE in phosphate buffer solution (pH 3.5). DPV parameters were selected as: pulse amplitude: 50 mV, pulse width: 50 ms, scan rate: 20 mV/s.

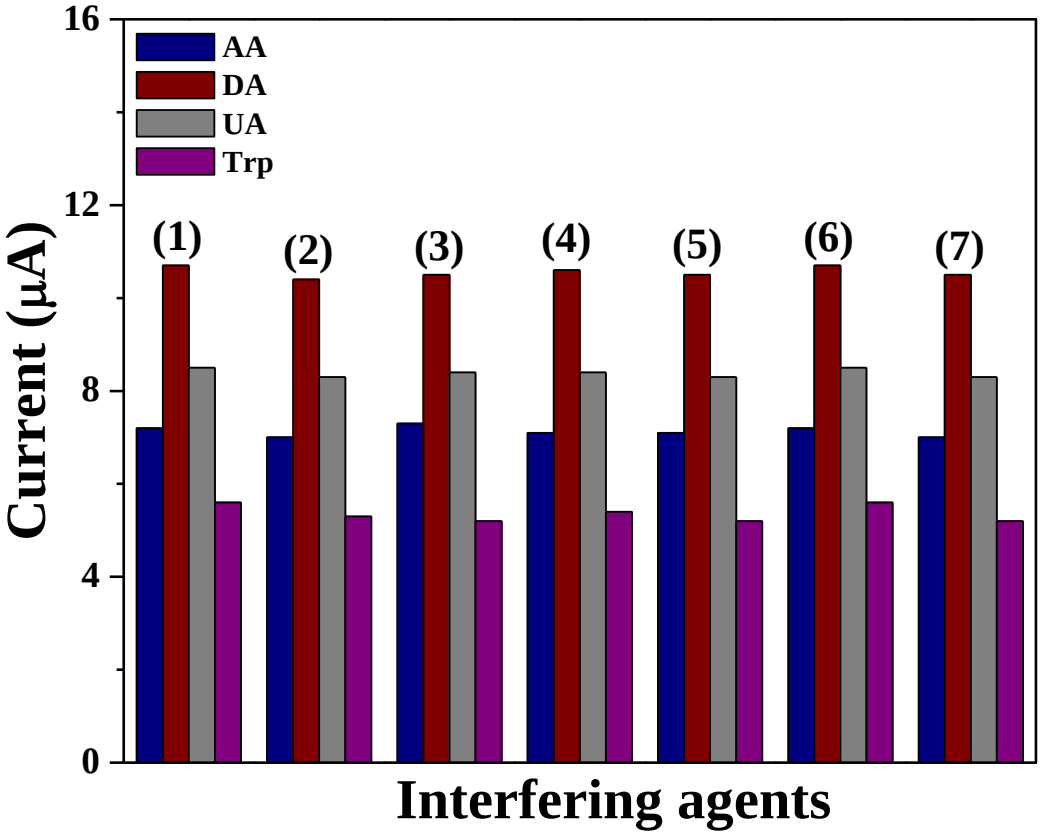

Fig. S11. The current responses at $NiCo_2O_4$ (30 %)/Nano-ZSM-5/GCE in phosphate buffer solution (pH 3.5) in the presence of (1) AA (10 μM), DA (10 μM), UA (10 μM), and Trp (10 μM) alone; (2) AA (10 μM), DA (10 μM), UA (10 μM), Trp (10 μM), and Na^+ (1200 μM); (3) AA (10 μM), DA (10 μM), UA (10 μM), Trp (10 μM), and K^+ (1200 μM); (4) AA (10 μM), DA (10 μM), UA (10 μM), Trp (10 μM), and Mg^{2+} (1200 μM); (5) AA (10 μM), DA (10 μM), UA (10 μM), Trp (10 μM), and Zn^{2+} (1200 μM); (6) AA (10 μM), DA (10 μM), UA (10 μM), Trp (10 μM), and glucose (800 μM); and (7) AA (10 μM), DA (10 μM), UA (10 μM), Trp (10 μM) and citric acid (1000 μM).

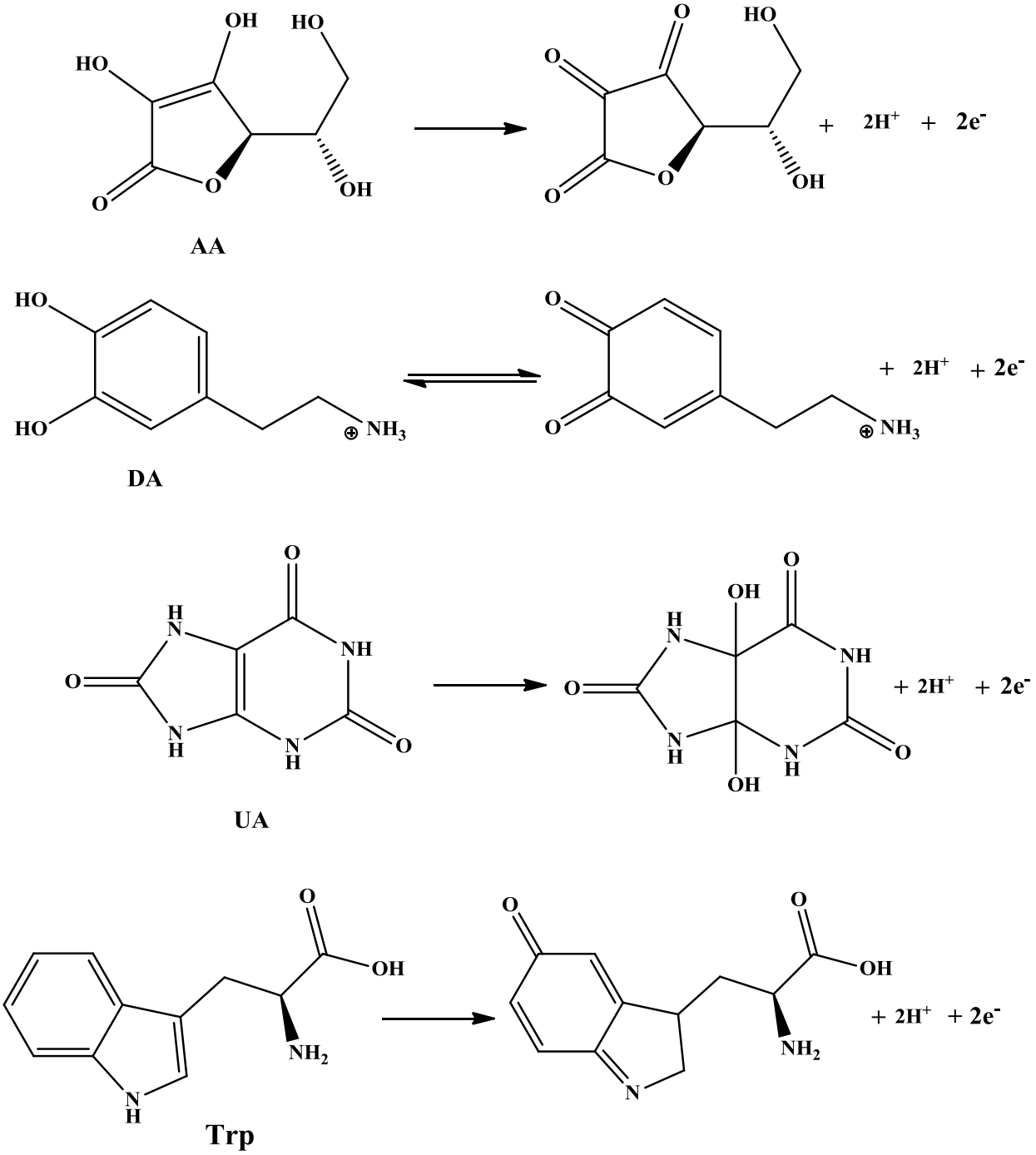

Scheme S1. Electrochemical oxidation of AA, DA, UA, and Trp at $NiCo_2O_4$ (30 %)/Nano-ZSM-5/GCE.

Table S1 Comparison of the electro-catalytic activity at various modified GCE in the simultaneous determination AA, DA, UA, and Trp.

S.No.	Modified Electrode	Analyte	Linear range (μM)	Detection limit (μM)	Sensitivity (μA/μM cm^2)
1.	$NiCo_2O_4$ (30 %)/Nano-ZSM-5/GCE	AA	1-1200	0.8	0.7
		DA	0.6-900	0.5	1.3
		UA	0.9-1000	0.7	1.0
		Trp	0.9-1000	0.7	0.6
2.	Nano-ZSM-5/GCE	AA	-	-	-
		DA	10-200	3.0	0.3
		UA	10-200	5.0	0.1
		Trp	10-200	4.0	0.2
3.	$NiCo_2O_4$/GCE	AA	12-400	8.0	0.2
		DA	10-200	7.0	0.3
		UA	10-200	9.0	0.2
		Trp	10-200	9.0	0.1
4.	ZSM-5/GCE	AA	-	-	-
		DA	10-200	9.0	0.2
		UA	10-200	10	0.2
		Trp	10-200	9.0	0.1

Table S2 Comparison of $NiCo_2O_4$ (30 %)/Nano-ZSM-5/GCE with other electrodes reported in the literature for AA, DA, UA, and Trp detection.

S.No.	Modified electrode	Analyte	Linear range (μM)	Detection limit (μM)	Reference
1.	GS–PTCA	AA DA UA Trp	20–420 0.4–370 4–540 0.4–140	5.60 0.13 0.92 0.06	[3]
2.	GNPs/PImox	AA DA UA Trp	210–1010 5–268 6–486 3-34, 84-464	2.0 0.08 0.5 0.7	[4]
3.	Fe(III)P/MWCNTs	AA DA UA Trp	14–2500 0.7–3600 5.8–1300 -	3.00 0.09 0.30 -	[5]
4.	MWCNT–FeNAZ-CH	AA DA UA Trp	7.77–833 7.35–833 0.23–83.3 0.074–34.5	1.11 1.05 0.033 0.011	[6]
5.	MWNTs/MGF	AA DA UA Trp	100–6000 0.3–10 5-100, 300-1000 5-30, 60-500	18.28 0.06 0.93 0.87	[7]
6.	Fe-Meso-PANI modified electrode	AA DA UA Trp	100-300 100-300 100-300 100-300	6.5 9.8 5.3 5.2	[8]
7.	AgNPs/rGO/GCE	AA DA UA Trp	10-800 10-800 10-800 10-800	9.6 5.4 8.2 7.5	[9]
8.	$NiCo_2O_4$ (30 %)/Nano-ZSM-5/GCE	AA DA UA Trp	1-1200 0.6-900 0.9-1000 0.9-1000	0.8 0.5 0.7 0.7	This work

GS–PTCA: hybrid of graphene sheets (GS) and 3,4,9,10-perylenetetracarboxylic acid (PTCA);
GNPs/PImox: gold nanoparticles/overoxidized-polyimidazole composite;
Fe(III)P/MWCNTs: chloro[3,7,12,17-tetramethyl-8,13-divinylporphyrin-2,18-dipropanoato(2-)] iron(III)/multi-walledcarbonnanotubes;
MWCNT–FeNAZ-CH: iron ion-doped natrolite zeolite–multiwalled carbon nanotube;
MWNTs/MGF: A multi-walled carbon nanotubes bridged mesocellular graphene foam;
Fe-Meso-PANI modified electrode: iron ion-exchanged mesoporous polyaniline;
AgNPs/rGO/GCE: Silver nanoparticles decorated reduced graphene oxide modified glassy carbon electrode

References

[1]	M. Sharp, M. Petersson and K. Edstrom, *J. Electroanal. Chem.*, 1979, **95**, 123-130.
[2]	Z. Galus, Fundamentals of Electrochemical Analysis, *Ellis Horwood, New York*, 1976.
[3]	W. Zhang, Y. Q. Chai, R. Yuan, S. H. Chen, J. Han and D. H. Yuan, *Anal. Chim. Acta*, 2012, **756**, 7-12.
[4]	C. Wang, R. Yuan, Y. Q. Chai, S. H. Chen, F. X. Hu and M. H. Zhang, *Anal. Chim. Acta*, 2012, **741**, 15-20.
[5]	C. Wang, R. Yuan, Y. Q. Chai, S. H. Chen, Y. Zhang, F. X. Hu and M. H. Zhang, *Electrochim. Acta*, 2012, **62**, 109-115.
[6]	M. Noroozifar, M. K. Motlagh, R. Akbari and M. B. Parizi, *Biosens. Bioelectron.*, 2011, **28**, 56-63.
[7]	H. Li, Y. Wang, D. Ye, J. Luo, B. Su, S. Zhang and J. Kong, *Talanta*, 2014, **127**, 255-261.
[8]	M. U. Anu Prathap and R. Srivastava, *Sens. Actuators, B*, 2013, **177**, 239-250.
[9]	B. Kaur, T. Pandiyan, B. Satpati and R. Srivastava, *Colloids Surf., B*, 2013, **111**, 97-106.